Study of Distortion and Residual Stresses on Friction Stir Welded 7075-T6 Aluminum Plates

Prepared by:
Beau White
Undergraduate, Mechanical Engineering

Faculty Advisors:
Dr. Michael West
REU Site Director, Department of Materials and Metallurgical Engineering

Dr. Damon Fick
Assistant Professor, Department of Civil and Environmental Engineering

Dr. Alfred Boysen
Professor, Department of Humanities

Program Information:
National Science Foundation

Research Experience for Undergraduates
Summer 2010

South Dakota School of Mines and Technology
501 E Saint Joseph Street
Rapid City, SD 57701

Abstract

The objective of this project is to investigate distortion in friction stir welded stiffened panels and also the residual stresses caused by this process. Distortion is a common problem experienced in friction stir welded stiffened panels. There are many factors that influence distortion and may be categorized as design-related and process-related variables. Significant design-related variables include the type of weld joint, plate thickness, thickness transition if the joint consists of plates of different thickness, stiffener spacing, and clamping. Important process-related variables are the travel speed, rotational speed, forge force, and welding sequence. A better understanding of how these parameters affect weld quality could lead to processes which eliminate the distortion in friction stir welded panels. Preliminary testing in 0.25-in thick 7075 aluminum plates showed that the location of clamping has a definite effect on strain produced (Shi 2008).

This project will use FARO arm data collected from a ½ inch grid on the specimen. FARO arm data will be processed with the MATLAB software programming; this will give us more flexibility in the presentation of the data as well as a savings in time since all graphs are generated automatically for a set of input data. The specimens used for this experiment are 0.040 inch thick 7075-T6 Aluminum plates. The dimensions are 4inches long and 8 inches wide. By welding two of these specimens together and observing the distortion caused by the FSW process we can get a better understanding of the behavior of the aluminum plates. This type of aluminum is used for aircraft and aerospace technologies due to its lightness and toughness.

1. Introduction

This report begins with a review of Friction Stir Welding (FSW) and the type of distortions caused by this process. Friction stir welding has been around for over 15 years. Researchers have been trying to find a way to limit the distortions caused by FSW. Also there has been in depth studying of the residual stresses caused by FSW (Arbegast 2001). More and more people are using FSW in industry and little is known about the distortion and stresses caused by this process. This report will address both these topics in FSW. By understanding the types of distortions and stresses caused by FSW you can find ways to reduce these occurrences. Most distortions caused by FSW are of the "saddle shape" where concave bending happens in the longitudinal or transverse direction. This type of bending can cause industry welds on aircrafts to bend during production which leads to more time and money trying to correct this distortion. By understanding the residual stresses caused by this process ways to reduce distortion induced by FSW can be found.

2. Broader Impact

The study of the distortions and residual stresses caused by FSW is very limited. Although FSW has been in industry for over 15 years the understanding of distortions and residual stresses caused by this process is limited. By studying these characteristics we can find ways to reduce the distortion of FSW structures. The type of Aluminum alloys used in this experiment has the potential to benefit the aircraft and aerospace industries tremendously. Identifying parameters that affect the distortion in FSW may create many new opportunities to joining and repairing aluminum metal types. Most aircraft and aerospace vehicles use this aluminum alloy for their designs but due to the distortion caused to these alloys many more procedures are done to fix these distortions which are expensive and time consuming. If there is a way to eliminate these distortions the aircraft and aerospace industries could save money and time.

3. Procedure

3.1 Materials

Following is a list of materials used in the current experiment. These materials are the most vital ones used for this experiment.

7075-T6 Aluminum Panels (Figure 1), used for aircraft and aerospace technologies. The upper skins and spar caps of wings often are of 7075-T6 and 7178-T6, because the critical requirement is high compressive strength, and the structure generally is not critical in tension loading or fatigue. Boeing, a leading company in the aircraft industry, is interested in the behavior of these alloys under Friction Stir Welding.

Dimensions for Aluminum Plates:

- 8 inches long
- 4inches wide
- 0.040 inch thick

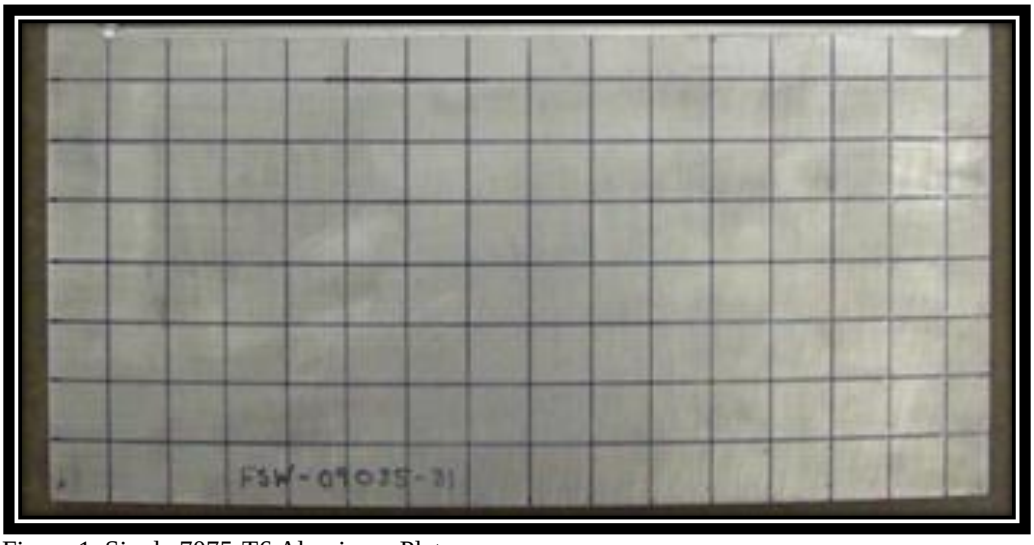

Figure 1. Single 7075-T6 Aluminum Plate.

CEA-13-120-EU Strain Gauges (Figure 2), Stress Analysis Gages. Thin, flexible gages with a cast polyimide backing and encapsulation featuring large, rugged, copper coated solder tabs. This construction provides optimum capability for direct lead wire attachment. Constantan alloy in self-temperature compensated form. 13 thermal expansion coefficient in ppm/°F. 120 Ohms in resistance. Primarily used for general-purpose static and dynamic stress analysis.

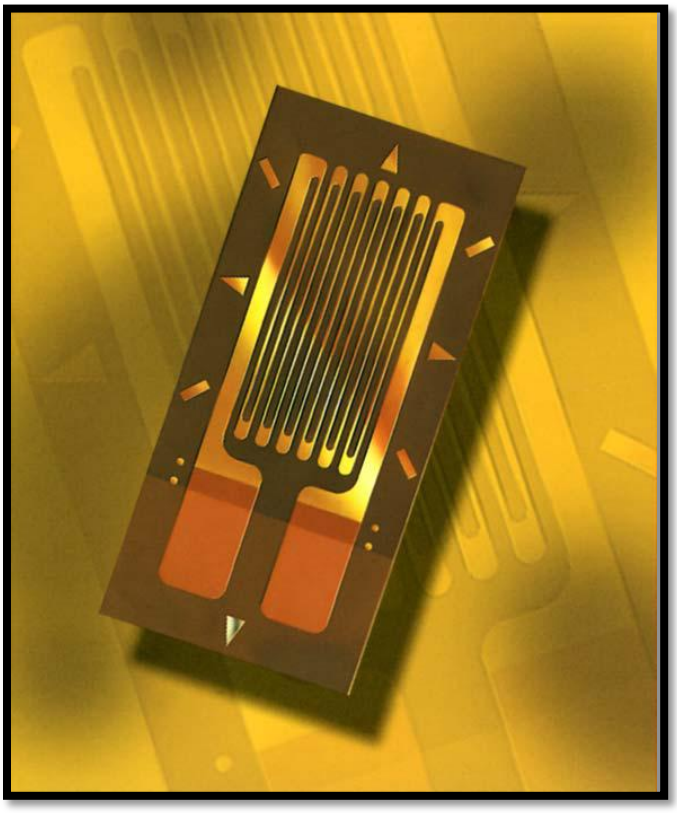

Figure 2. CEA-13-120-EU Strain Gauge.

3.2 Equipment

Following is a list of equipment used in the current experiment. These materials are the most vital ones used for this experiment.

MTS ISTIR 10 Gantry & Pin (Figure 3&4), Intelligent Stir Welder. This system is a 5-DOF system capable of producing parts requiring multi-axis welding capability. However, this system has a 10-ton forge load capacity, which is required for thicker section welds and non aluminums.

Figure 3. MTS ISTIR 10 Gantry at SDSM&T.

- Weld parameters
  - Traverse Speed – 10.0 ipm.
  - Rotational Speed – 1200 rpm, 900rpm, 600rpm.
  - Position Control
  - Weld Depth – 0.029 in.

Figure 4. Pin used for welding.

- Pin tool dimensions
    - Shoulder diameter – 0.249 in.
    - Pin diameter – 0.086 in.
    - Pin length – 0.029 in.

FARO arm (Figure 5), Position Measuring Device. The FaroArm is a tool for completing surface measurements and dimensional calculations to the highest degree of precision of approximately 0.001 inches. The system provides the ability to perform a CAD analysis, inspections, and alignments with ease.

Figure 5. Measurements being taken with FARO arm.

MATLAB 7.0 (Figure 6) **,** Matrix Analysis. A high-level language and interactive environment that enables you to perform computationally intensive tasks faster than with traditional programming languages such as C, C++, and Fortran.

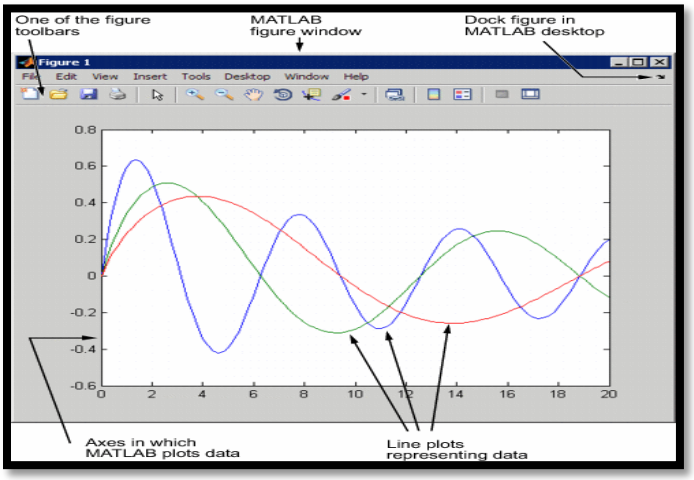

Figure 6. Graph produced on MATLAB.

3.3 Procedures

In order to start this experiment the 7075-T6 Aluminum plates must be prepared. First the plates are marked with ½ inch grids in the x and y direction on the surface of the plate for FARO arm measurements. Strain gauges must be attached to one of the panels and connected to the wires as pairs of panels will be welded. Panel diagrams showing the grids and strain gauge layout can be seen in Figure 7 and Figure 8.

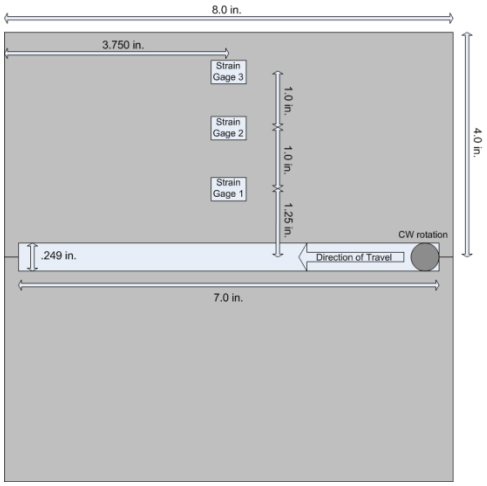

Figure 7. Panel layout.

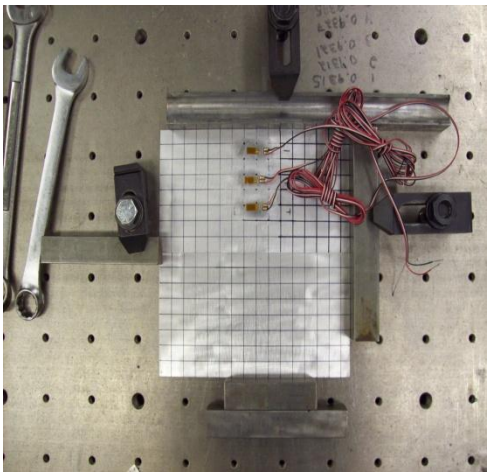
Figure 8. Actual picture of panel layout before weld.

The residual stresses will be measured using strain gauges that will be applied to the panels during the FSW process. CEA-13-120-EU strain gauges were used on the panels. One placed near the welding area, another towards the center of panel and another by the clamping area of the panel (Figure 8). The data gathered by the strain gauges will be processed using a Digit Acquisition (DAC) system showing the stresses in a graph.

Two panels are ready for welding as seen in Figure 8 clamp the two plates down for FARO arm measurements. Measure every intersection of the grids marked on the aluminum plates shown in Figure 9. This process is done right before and right after the weld is done. Paper shimms are used to reduce any deflection or movement of the plates during these measurements.

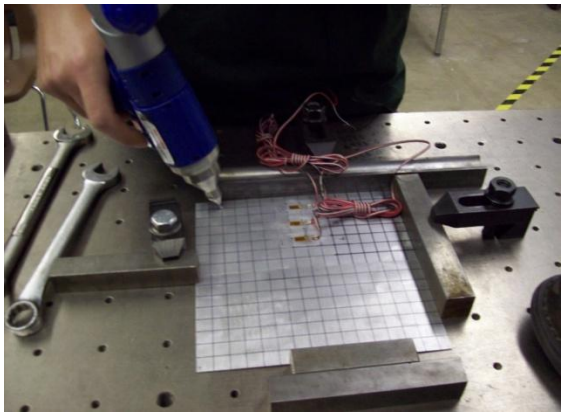

Figure 9. Measure intersection points using FARO arm.

Before welding the specimen the strain gauges need to be connected to the DAC system for recording the strain gauges data. With the specimens ready it is welded with the parameters listed in the equipment section. After the weld is finished, a second set of FARO arm measurements are made and the data is retrieved from the DAC system and FARO arm for analysis.

4. Results

4.1 Residual Stresses

Six specimens were welded; 09035-31, 09035-33, 09035-34, 09035-35, 09035-36, and 09035-37 the first four specimens using 1200 rpm for their rotational speed. Specimen 09035-36 and 09035-37 used 900rpm and 600rpm for their rotational speeds. The residual strains were recorded using the strain gauges and the DAC system. Below are the graphs from the DAC system and strain gauges. Figures 10-12 show the strain data for specimen 09035-34 as a function with time. Table 1 shows DAC system average strain data.

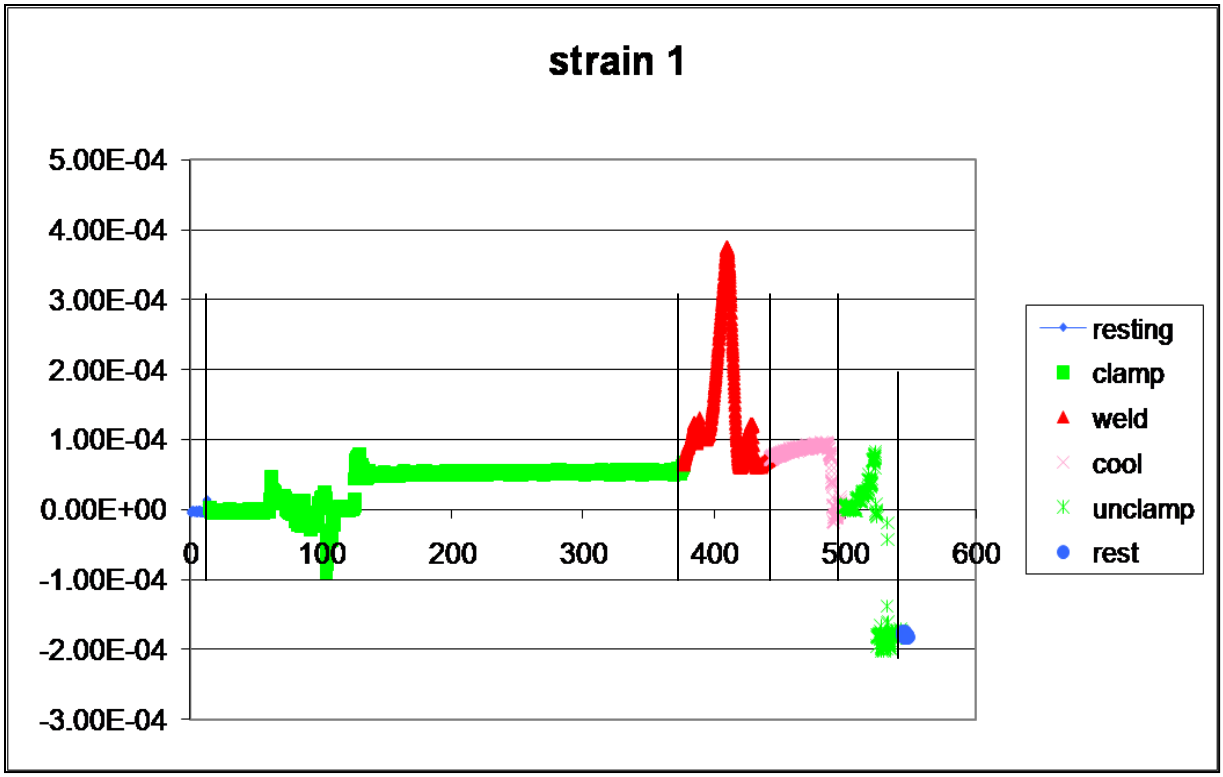

Figure 10. Strain Gauge 1 Data vsTime 09035-34.

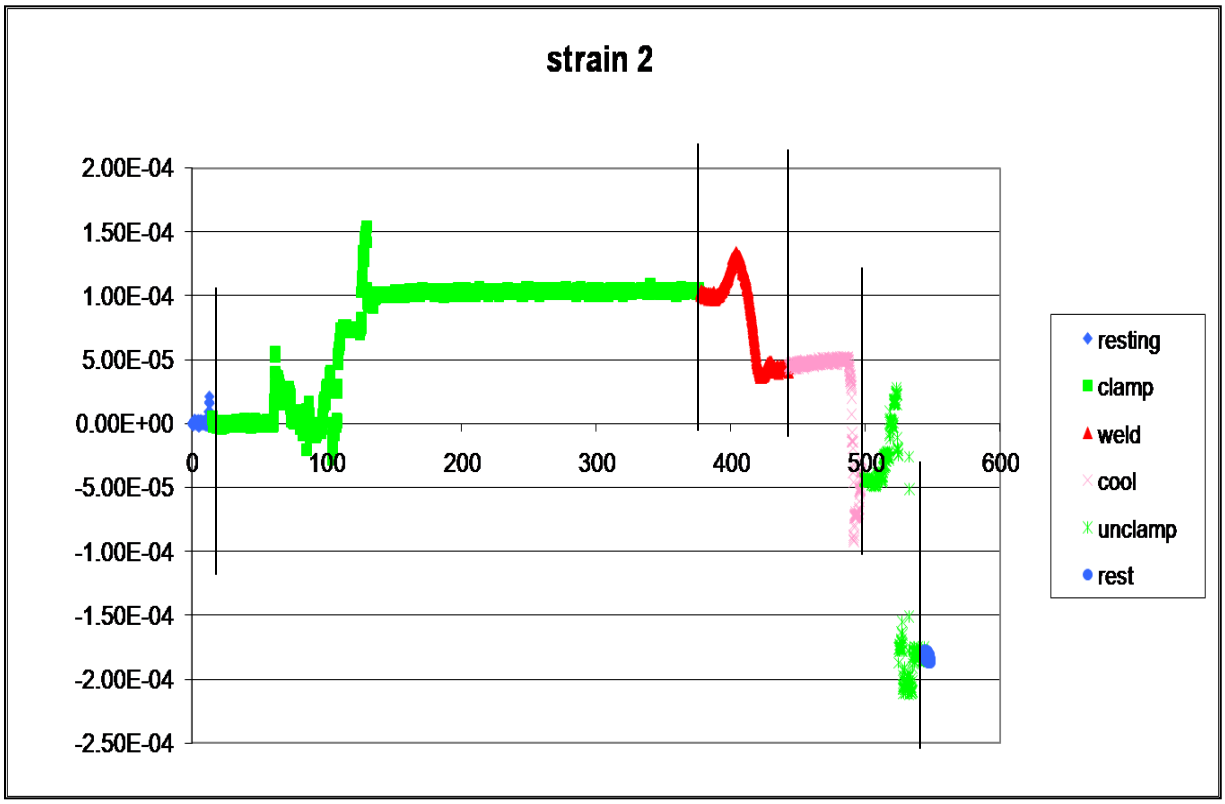

Figure 11. Strain Gauge 2 Data vs. Time 09035-34.

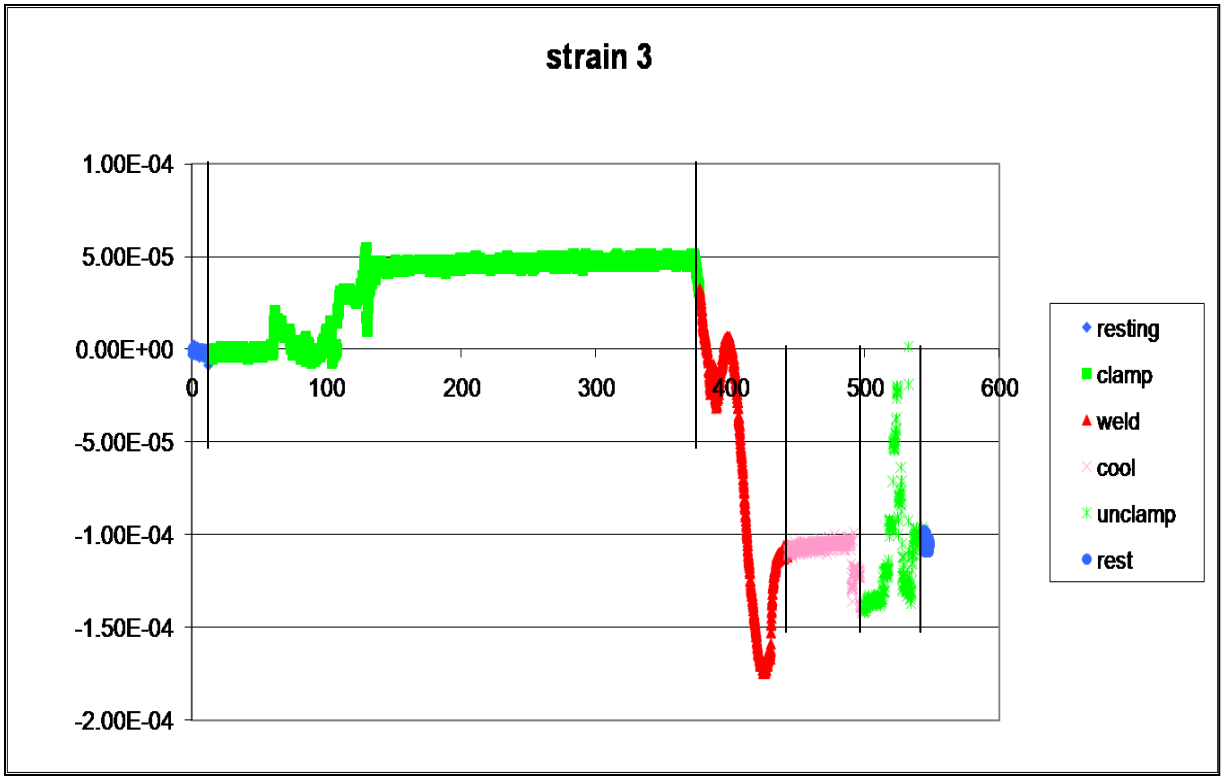

Figure 12. Strain Gauge 3 Data vs. Time 09035-34.

Specimen ID	Strain 1	Strain 2	Strain 3
FSW-09035-31	-4.10E-04	-4.60E-04	-4.30E-04
FSW-09035-33	5.07E-05	-2.36E-06	-4.67E-05
FSW-09035-34	-1.80E-04	-1.85E-04	-1.10E-04

Table 1. Strain Data Indicated by Data Acquisition System

4.2 Distortion

The distortion of the panels was measured using the FARO arm measurements taken before and after welding to visualize the measured distortion. The points measured by the FARO arm were applied to a program in MATLAB that would produce a 3-D graph of the actual pre and post weld positions of the panels. In Figures 13-26 the distortions caused by FSW are shown graphically.

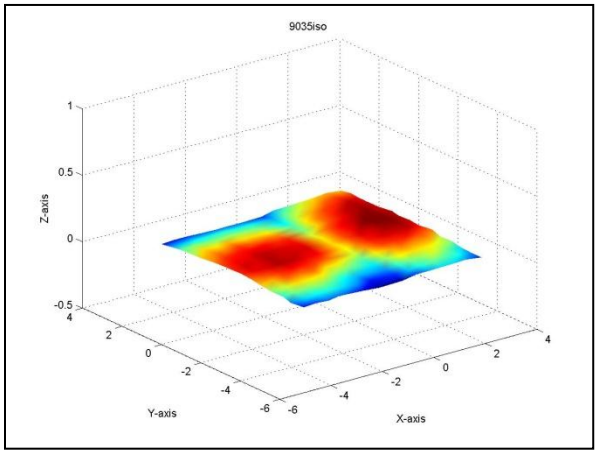

Figure 13. FARO mapping pre weld 09035-31.

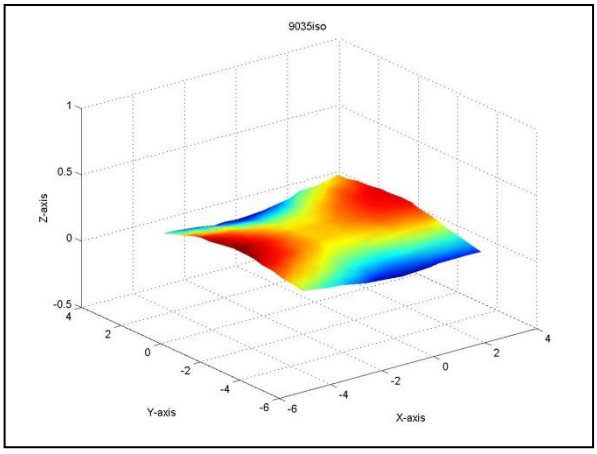

Figure 14. FARO mapping post weld 09035-31.

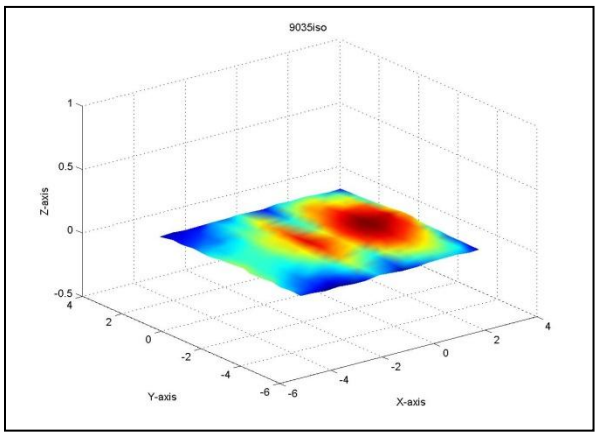

Figure 15. FARO mapping pre weld 09035-33.

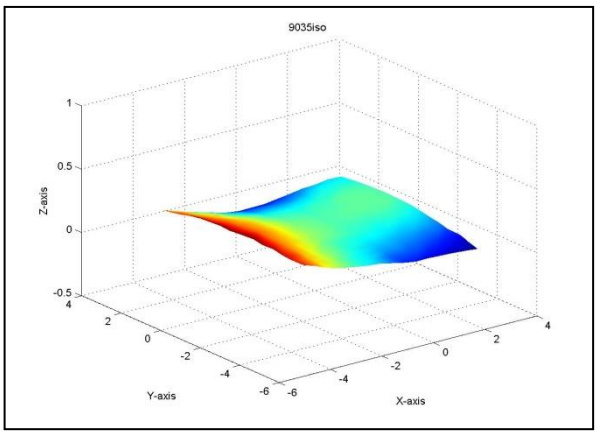

Figure 16. FARO mapping post weld 09035-33.

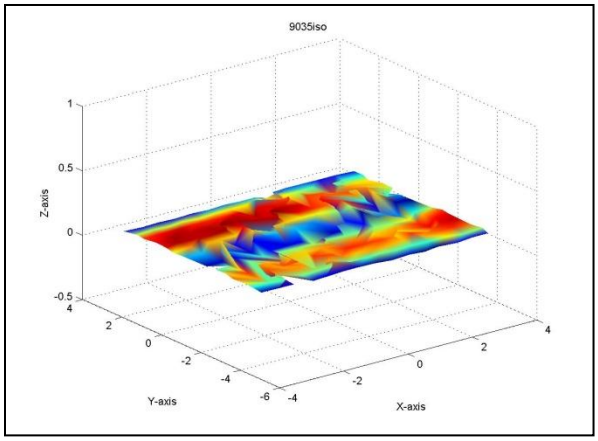

Figure 17. FARO mapping pre weld 09035-34.

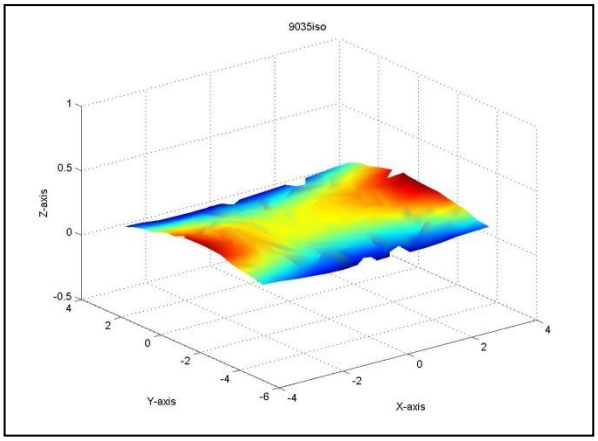

Figure 18. FARO mapping post weld 09035-34.

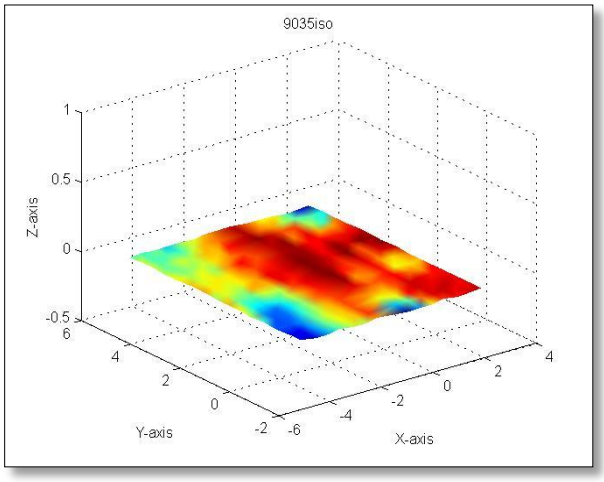

Figure 19. FARO mapping pre weld 09035-35.

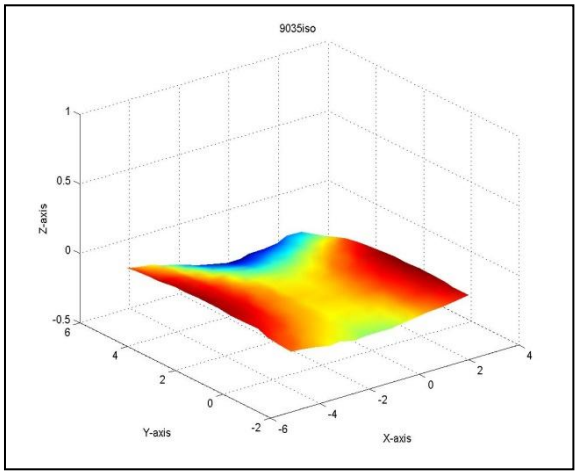

Figure 20. FARO mapping post weld 09035-35.

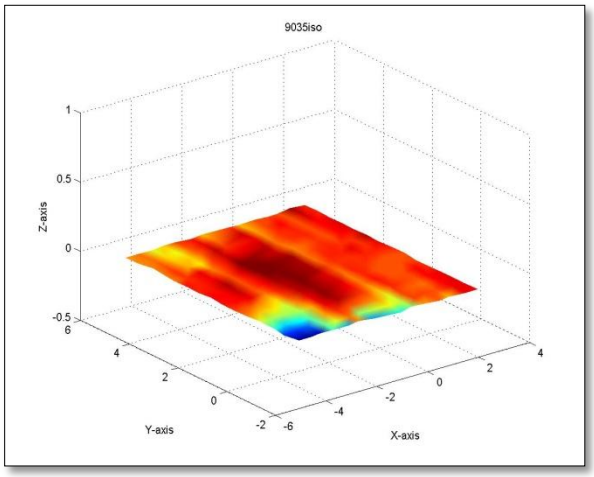

Figure 21. FARO mapping pre weld 09035-36.

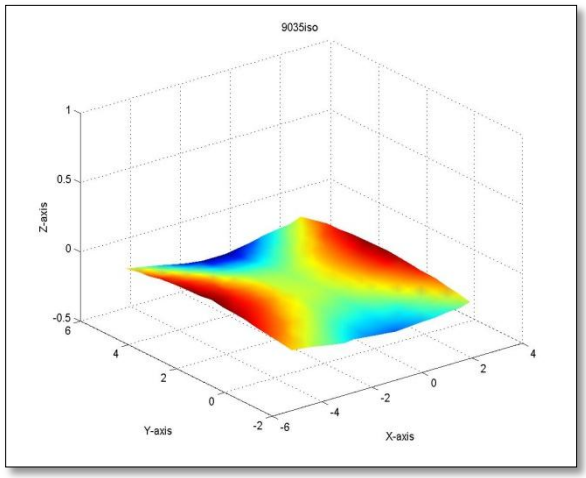

Figure 22. FARO mapping post weld 09035-36.

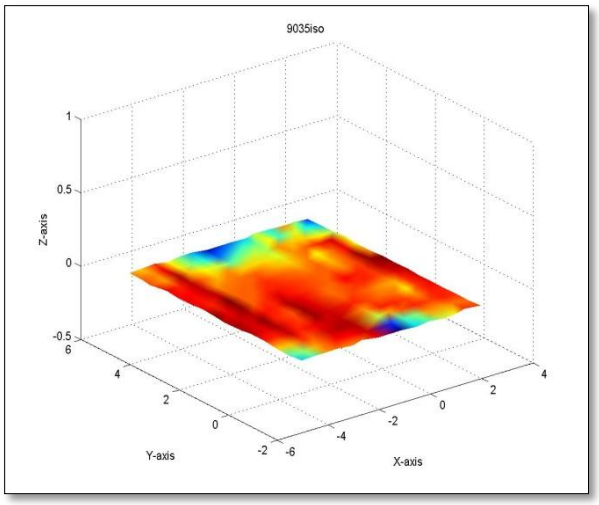

Figure 23. FARO mapping pre weld 09035-37.

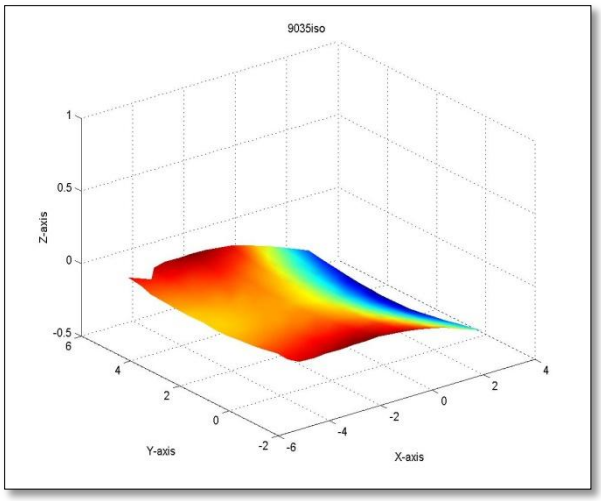

Figure 24. FARO mapping post weld 09035-37.

By changing the scale on the z-axis graphs are generated that magnify the actual contour and shape of the surface. In figures 25-26 the Z-axis is exaggerated to show how much the surface is distorted visually this exaggeration is done to the specimen 09035-31.

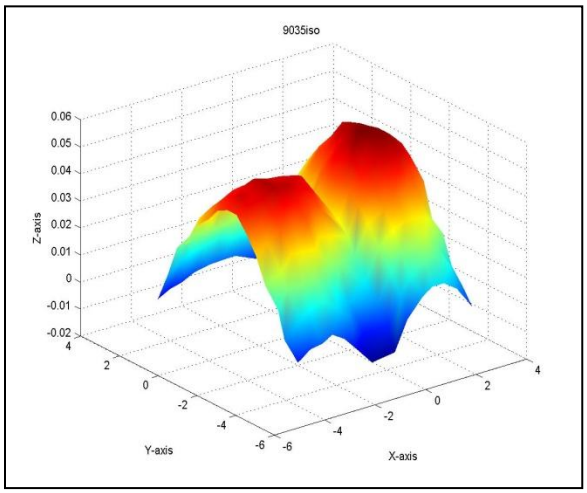

Figure 25. 09035-31 Scale manipulation pre weld.

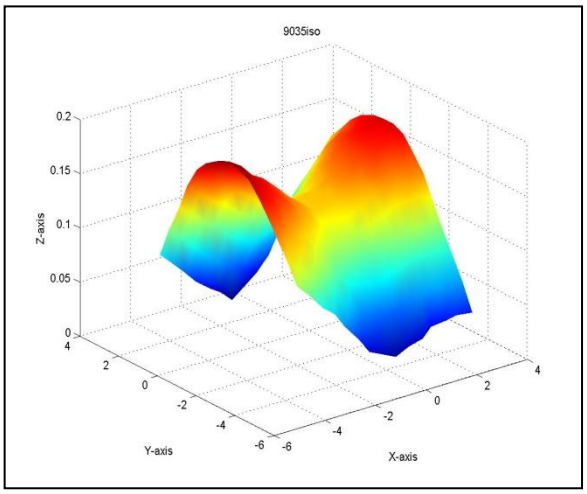

Figure 26. 09035-31 Scale manipulation post weld.

5. Discussion

5.1 Strain Calculation

After the strain data was recorded by the DAC system two methods were used to attempt to calculate the strain using the FARO arm data and are listed below:

1. Pick 3 points in proximity of strain gauge and estimate curve length at surface by finding the equation for a circle for the three points and determining the change in curve length from data before and after the weld.
2. Using Excel, an equation for a curve that provides a best fit was identified. Calculus was used to find the length of the curve between the extremities of the strain gauge before and after welding.

The first method used the calculation for strain gauge 3 on specimen 09035-31 was approximately 3.5704 when compared to the strain gauge 3 data on 09035-31 from Table 1 which is approximately -4.30E-04 there is a significant amount of error over 100% produced using that method.

The second method graphed the FARO data at the location of the strain gauges and found the equations of arc using excel (Figure 21). The derivatives were calculated in MathCAD. The strain was calculated by finding the change in arc length and comparing that to the strain data in Table 1. The equation used was;

$$S = \int_b^a \sqrt{1 + \left(\frac{dy}{dx}\right)} \, dx$$

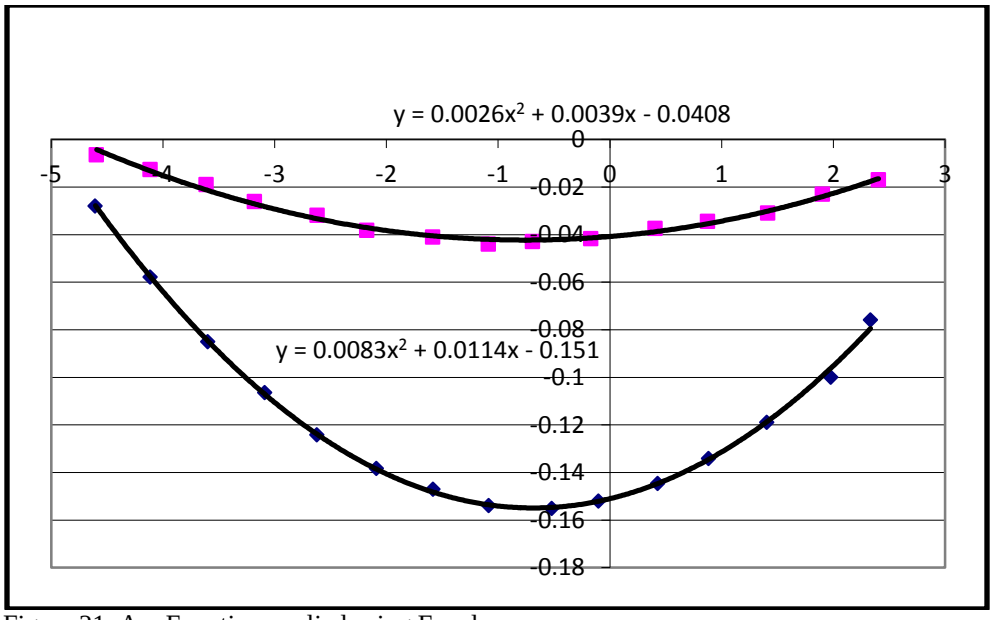

Figure 21. Arc Equation applied using Excel.

This method's results in comparison to the strain data from Table 1 was around a 50-100% error. By looking at the strain graphs (Figures 10 – 12) you can clearly see that clamping of the specimens causes a significant amount of strain to be applied to the specimens. Clamping produces enough strain to be considered a significant variable in distortion of these aluminum plates.

5.2 Distortion Quantification

The errors obtained in the attempted calculation of strains from the FARO arm data (50-100%) were too high for the accurate quantification of distortion in the FSW process. These errors are believed to be from the inability to place the FARO arm probe in the exact location for the before and after welding measurements. A different method was investigated in an attempt to more accurately quantify distortion.

After the plates were welded there was two methods used to calculate a "distortion index" to quantify the distortion;

1. Sum the absolute values of the difference between initial and final Z-axis positions of the welded specimen.
2. Taking the derivatives (slope) of curve fitted equations from the FARO arm data at opposite ends of the plate.

The first method applied used the equation;

$$D=\Sigma|Zi-Zf|$$

This calculation was done using Excel Table 2.

Z-axis Position	
Specimen	Distortion Index
09035-31	20.15
09035-33	25.11
09035-34	17.42
09035-35	17.47
09035-36	16.67
09035-37	23.53

Table 2. Excel Distortion Indices.

By studying these indices and the overall distortion of the plates visually and graphically the resulting indices seem to an appropriate fit for quantifying the distortion. Specimen 09035-33 had the highest index and visually was the plate that distorted the most. Also specimen 09035-36 distorted the least visually and had the lowest index. So this index method can be used to quantify distortion in simple distortion cases.

The second method used the derivative approach. The objective of this method is to quantify distortion in a plate as the result of friction stir welding, however it could be used in a

variety of situations. This method was developed as a result of the need for a way to quantify distortion in welded plates when only topographical information is provided.

The derivative method that is being used to quantify distortion is used through the use of curve fitting and differences in the first derivative (slope) at opposite ends of the plate. There are methods for dealing with complex surfaces but for our purposes the simplified version will work.

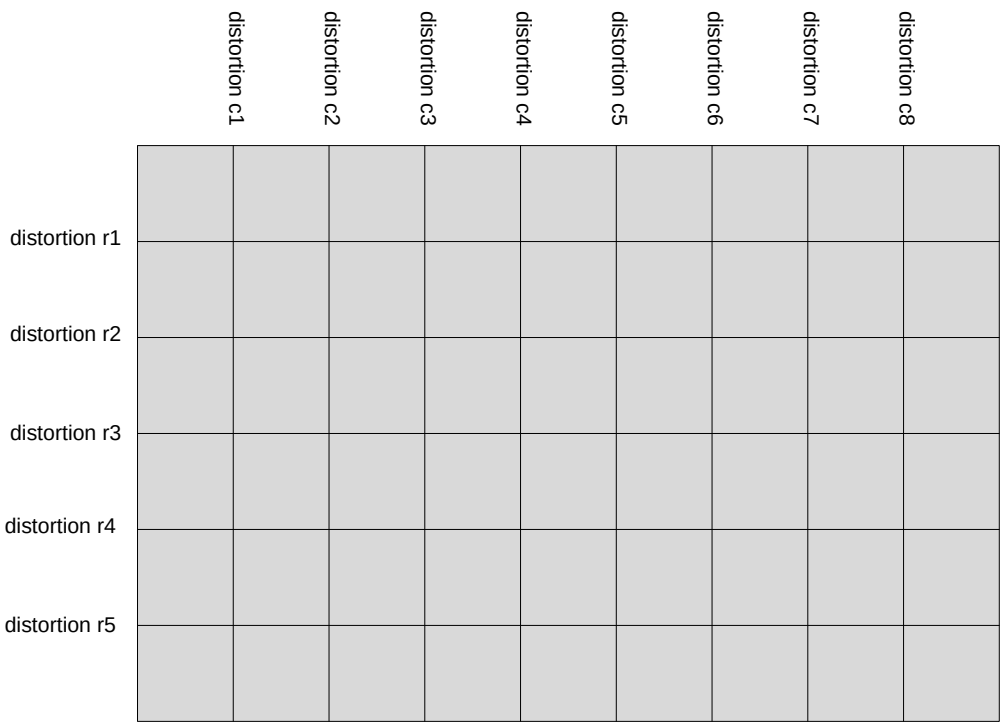

$$distortion\ row/column\ \# = \left| \frac{\frac{dz}{dx_i} - \frac{dz}{dx_f}}{x_i - x_f} \right|$$

The result of this equation is that the total change in gradient for the row/column is measured as $\frac{\Delta\frac{dz}{dx}}{in.}$. The summation of all rows and columns gives a hypothetical and untested result which may be used as an index to total distortion where

$$Arbegast\ Index = \sum distortion\ in\ rows + \sum distortion\ in\ columns$$

More complex curves require calculation of the second derivative of each row/column gradient curve and determination of the inflection points in each curve. The curve is then subdivided into simple curves which are then fit with curves which are degree 2 polynomials and the above process is then performed with the result for each row/column = summation of results.

This method's values are shown in Table 3. Studying these indices and the overall distortion of the plates visually and graphically the resulting indices seem to an appropriate fit for quantifying the distortion. Specimen 09035-33 had the highest index and visually was the plate that distorted the most. Also specimen 09035-36 distorted the least visually and had the lowest index. This index method can be used to quantify distortion in more complex distortion cases.

With the two welded specimens 09035-36 and 09035-37 they used different rotational speeds of 900rpm and 600rpm. By welding these two specimens with different rotational speeds than the other four we hoped to achieve a distortion pattern related to rotational speed. However since the distortion index for specimen 09035-37 fell in between the values for the 1200 rpm welded specimens the pattern is indistinguishable and it shows that rotational speed plays a small role in the overall distortion of these plates.

6. Conclusion

6.1 Summary

Studying the distortion caused by Friction Stir Welding can lead to FSW being the leading process in joining and welding technology. Finding a way to reduce these distortions can ultimately save the aircraft and aerospace industry time and money spent on correcting these distortions. Mapping the position with the FARO arm before and after welding shows the distortion visually. However trying to use this data for strain correlation between strain gauges and recorded positions from FARO arm is inconsistent and produces too much error when calculated with the two techniques mentioned above. Studying the strain versus time graphs shows that clamping produces enough strain to be considered a significant parameter in distortion of aluminum plates. Two methods discussed above for quantifying distortion are justifiable for use as indices in distortion. The Z-axis displacement method can be used in simple cases of distortion and the derivative method can be used in more complex cases of distortion. Rotational Speed plays a small role in the overall distortion of these aluminum plates.

6.2 Future Work

Further testing of specimens with different welding parameters such as; rotational speed, traverse speed, clamping, specimen length, specimen thickness, specimen width, and loads can give us a more in depth look to what parameters effect distortion in different ways. By studying these different parameters a procedure can develop to ultimately reduce the distortion caused by Friction Stir Welding.

References

1) Shi, Q.-Y. (2008). Experimental study on distortion of al 6013 plates after friction stir welding. *Science and Technology of Welding and Joining*, *13*(5), 472-479.
2) Larose, S. (2010). Limitation of distortion in friction stir welded panels using needle peening. *Materials Science Forum*, *638-642*, 1203-1208.
3) Bhide, S.R. (2006). Comparison of buclking distortion propensity for saw, gmaw, and fsw. *Welding Journal*, *85*(9), 189-195.
4) Posada, M. (2006). Friction stir welding advances joining technology. *AMPTIAC Quarterly*, *7*(3), 13-20.
5) Teng, Tso-Liang. (2001). Analysis of residual stresses and distortions in t-joint fillet welds. *International Journal of Pressure Vessels and Piping*, *78*, 523-538.
6) Arbegast, W.J. (2001). Distortion and residual stress analysis of friction stir welded 2195 al-cu-li plates. *Lockhead Martin Michoud Space Systems* , 1-6.
7) Xu, J. (2007). Effect of vibratory weld conditioning on the residual stresses and distortion in multipass girth-butt welded pipes. *International Journal of Pressure Vessels and Piping*, *84*, 298-303.
8) Owen, R.A. (2003). Neutron and synchrotron measurements of residual strain in tig welded aluminium alloy 2024. *Materials Science and Engineering*, *A346*, 298-303.
9) Milan, M.T. (2007). Residual stress evaluation of aa2024-t3 friction stir welded joints. *Journal of Materials Engineering and Performance*, *16*(1), 86-92.
10) Leggatt, R.H. (2008). Residual stresses in welded structures. *International Journal of Pressure Vessels and Piping*, *85*, 144-151.
11) Tseng, K.H. (2003). The Study of nitrogen in argon gas on the angular distortion of austenitic stainless steel weldments. *Journal of Materials Processing Technology*, *142*, 139-144.
12) Tsai, C.L. (1999). Welding distortion of a thin-plate panel structure. *Welding Research Supplement*, 156s-165s.

Acknowledgements

The funding for this research came from the National Science Foundation. Thanks to advisors Dr. Damon Fick, Dr. Bharat Jasthi, and REU site director Dr. Michael West for their guidance, Dr. Alfred Boysen for his critique in writing and speaking, special thanks to students James Haiston and Matthew Deardoff for the valuable input to this research project, faculty and staff at SDSM&T and the students working in the Advanced Material Processing Center for their help.